Self-Healing of Internal Damage in Synthetic Vascular Materials

By *Andrew R. Hamilton, Nancy R. Sottos,** and *Scott R. White**

Inspired by natural healing processes, a variety of synthetic self-healing materials have been developed that can heal structural damage autonomously.[1] Artificial vascular systems, which enable multiple healing cycles, have been successfully incorporated into materials with low load bearing requirements to heal cracks in coating materials and skin-core debonding with foam crushing in composite sandwich structures.[2–9] The healing strategy in these previous demonstrations mimics that of human skin, in which a minor cut triggers blood flow from the capillary network in the underlying dermal layer to the wound site (**Figure 1a,b**). Cracks are confined to the coating material or near the skin-core interface; the vascular system is intentionally placed within regions with a low probability of failure and terminates where damage is expected to occur. Here, we explore the interaction of cracks with a vascular system embedded in a bulk structural material. In contrast to prior investigations, the integrity of the vascular network is compromised and its connectivity disrupted by the damage. Although there has been discussion of optimal vascular designs for structural materials,[10–14] we demonstrate the ability to repeatedly repair large damage volumes within a vascularized structural material for the first time.

The healing response of this synthetic system resembles the early stages of clotting and hard callous formation in bone injuries (Figure 1c,d). Healing in cortical bone begins when the disruption of blood vessels leads to clotting and the formation of a hematoma that encloses the injury (Figure 1c). The hematoma gradually mineralizes with hydroxy apatite to form a hard callus of woven bone. Angiogenesis–guided by the location of pre-existing blood vessels–begins in the early stages of healing, maintaining vascular connections across the injured area.[15] Eventually woven bone is replaced by lamellar bone, which adapts to its service loads according to Wolff's law.[16–19] In addition, the presence of vascular canals in cortical bone increases the bulk material toughness by deflecting crack propagation and promoting crack-bridging and microcracking.[20]

A new experimental protocol was implemented for assessing the healing of damage within a vascularized polymer. We adopted the double cleavage drilled compression (DCDC) fracture sample geometry[21–24] (**Figure 2a**) in order to initiate stable crack growth and ensure crack arrest before catastrophic sample failure. When the DCDC sample is compressed, two nominally symmetric cracks grow from the crowns of the central hole in a stable fashion. Using the model developed by Plaisted et al.[23] the fracture toughness of the specimen was determined based on the sample dimensions and the applied compressive stress necessary for crack propagation. (See Supporting Information for details on sample analysis.)

Self-healing, microvascular DCDC samples were manufactured in an epoxy matrix with channels 200 μm in diameter using direct-ink writing with dual ink deposition.[4,5,7] The vascular architecture of the final part, detailed in Figure 2a, was designed to distribute two fluids throughout the volume of the material. The two components of the healing chemistry, epoxy resin (Epon™ 8132) and aliphatic amidoamine hardener (Epikure™ 3046), were injected into alternating layers of microchannels. This two-part epoxy healing system was selected based on the evaluation previously conducted by Toohey et al.[6] The components are low viscosity and have a stoichiometric ratio (2.2:1) that is comparable to the alternating layout of microchannels through the thickness of the sample (3:2). Because each layer of microchannels is isolated, the healing components did not come into contact until a fracture event intersected both a resin-filled and a hardener-filled microchannel. Vascularized control samples were identical to self-healing samples, but contained either resin alone or hardener alone within the entire vasculature. Neat samples with no microchannels were also fractured and subjected to the same testing protocol as self-healing samples to verify that the matrix material did not heal inherently or undergo any change (e.g. further crosslinking) that might be attributed to healing.

After loading to fracture, healing agents flowed into the crack plane through capillary action and were visualized with fluorescent dyes (Figure 2b and Video S1, Supporting Information). The alternation between resin and hardener-filled channels through the thickness of the sample resulted in multiple interfaces between the resin and hardener in the crack plane, providing a more favorable condition for diffusional mixing of the two components.

Representative plots of normalized average crack length (l/R) as a function of applied compressive stress are shown in **Figure 3a**, along with model predictions. The applied stress necessary for crack growth increases while the crack tip is close to the hole, and reaches a constant value at longer crack lengths ($l/R > \sim 0.75$). Vascularized samples behaved similarly to neat samples (with

[*] Prof. N. R. Sottos
Materials Science and Engineering Department
University of Illinois at Urbana-Champaign
Urbana, IL 61801 (USA)
E-mail: n-sottos@illinois.edu
Prof. S. R. White
Aerospace Engineering Department
University of Illinois at Urbana-Champaign
Urbana, IL 61801 (USA)
E-mail: swhite@illinois.edu
A. R. Hamilton
Mechanical Science and Engineering Department
University of Illinois at Urbana-Champaign
Urbana, IL 61801 (USA)

DOI: 10.1002/adma.201002561

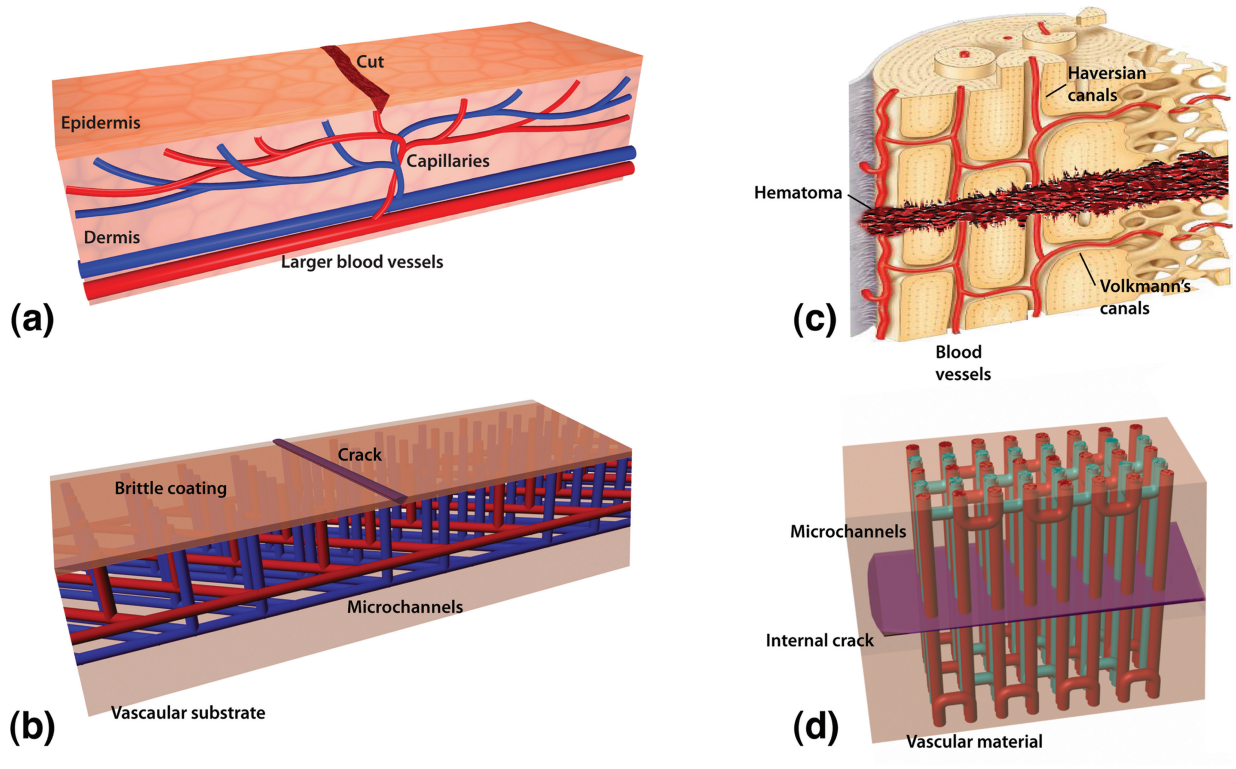

Figure 1. Schematics of surface damage being healed in a) the epidermal layer via the vascularized dermis (Reprinted with permission.[2] Copyright 2007, Macmillan) and b) a brittle coating material via an interpenetrating vascular network within a substrate (Reproduced with permission.[7]) Schematics of internal damage being healed (c) in cortical bone (image adapted with permission.[25] Copyright 2007, Pearson Benjamin Cummings) and d) within a synthetic vascular material.

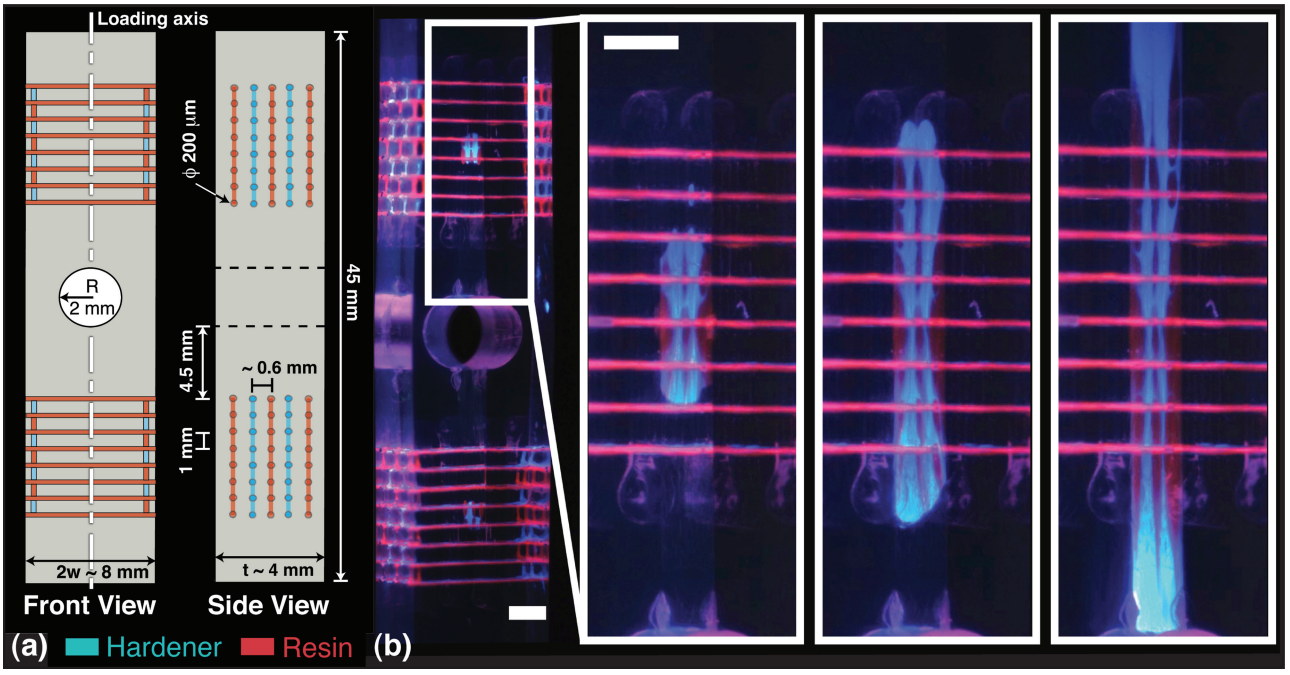

Figure 2. a) Microvascular DCDC sample geometry and vascular design (not drawn to scale). b) Evolution of healing agents (resin and hardener) released into the crack plane of a fractured DCDC sample. Resin and hardener were dyed with Nile red and perylene, respectively. Scalebars are 2 mm.

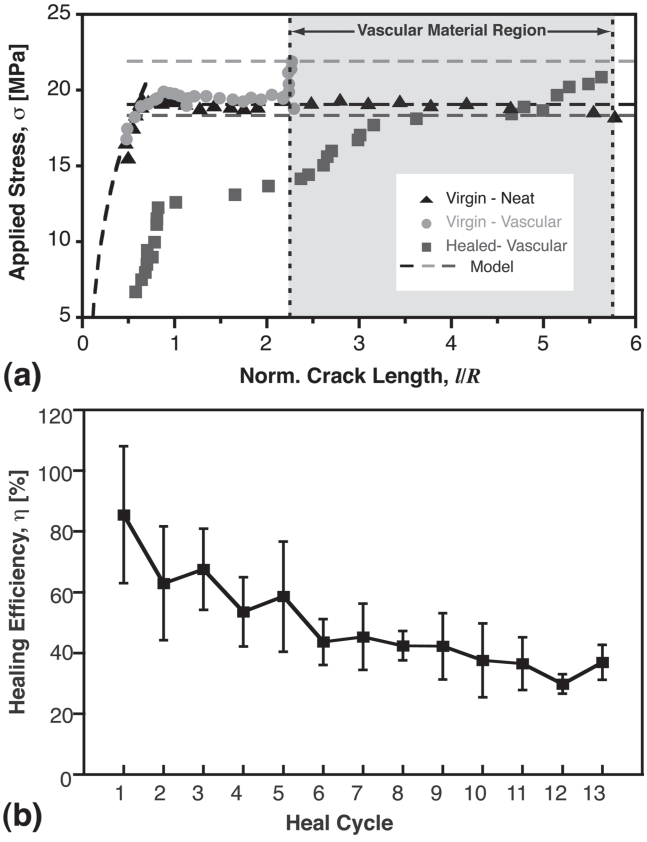

Figure 3. a) Applied stress necessary for crack propagation in a neat control sample, a virgin vascular sample, and a healed vascular sample. The model fit for each sample is plotted as a dashed line. (b) Average healing efficiencies for vascular samples with error bars bounding one standard deviation of error (see Table S1 for healing data).

no vasculature) until the cracks intersected the first bank of microchannels (at a normalized crack length of $l/R = 2.25$). After intersecting the microchannels, the crack tip was pinned and propagation halted until the applied stress exceeded a level that was sufficient to overcome the pinning mechanism. Crack propagation was typically unstable after this point (hence no data points were obtained after the first microchannel position in Figure 3a), but crack arrest occurred before complete cleavage of the sample.

The mode I critical stress intensity factor (K_{IC}) was evaluated by fitting the model to the experimental data in the region of constant applied stress for crack propagation. The virgin fracture toughness of vascularized samples was calculated by fitting the constant-stress portion of the model through the maximum stress (where the crack tip was pinned on the microchannels). For consistent healing assessment, fracture toughness after healing was evaluated by fitting the model to the maximum stress plateau exhibited through the vascularized portion of the material ($2.25 < l/R < 5.75$). The vascular sample data in Figure 3a (both virgin and healed) did not exhibit the ideal stress plateau predicted by theory. This non-ideal behavior is likely due to variations in material properties that exist along the length of the crack that are caused by either vascular features (in virgin tests), or non-uniform curing (in healed tests). Therefore, the calculated fracture toughness is spatially dependent and a function of position along the crack path. The healed material with the highest fracture toughness tended to occur within the region of vascularized material, where the healing agents were most directly supplied to the crack.

Internal damage in our synthetic vascular material, analogous to the type of damage observed in bone, was healed through multiple cycles of damage and healing. The healing efficiency (η) was calculated as the ratio of the healed sample fracture toughness to that of the virgin sample. Even though the crack fully penetrated the vascular network, the samples achieved remarkable healing efficiencies on par or superior to that observed previously for coatings in which the vascular substrate remained undamaged.[6,7] A summary of healing results is presented in Figure 3b, in which the average healing efficiency is plotted for each cycle of damage and recovery. The average recovery of fracture toughness on the first healing cycle was 86% of the virgin sample fracture toughness, with a maximum of 120% and a minimum of 61% (the full data set is given in Table S1, Supporting Information). In subsequent healing cycles, the average healing efficiency tended to decrease, as did the number of samples that continued to heal. Control samples confirmed that this recovery is due to curing of the healing chemistry in the crack plane. Over 13 healing cycles were obtained for the best samples, demonstrating that large scale damage to a structural material can be healed repeatedly by an embedded microvascular network.

The major factor limiting the performance of the network was the eventual blockage of microchannels caused by continuous build up of healed material in the crack plane after many cycles of loading. This phenomenon was observed qualitatively while refilling the microchannels before each fracture test. Examination of the fracture surfaces after 10 healing cycles (**Figure 4**) provided evidence that the healed epoxy film formed by reaction of the healing agents covered many of the microchannels. The incomplete coverage of healed material in the crack plane, also shown in Figure 4, is the likely explanation for the observed deviation from the predicted behavior of constant stress for crack propagation in healed samples (Figure 3a).

Uniform flow of both the resin and hardener is necessary to provide a sufficient distribution of both components in the crack plane. Since the flow is not controlled, but rather driven by capillary action and surface forces, small differences in crack separation and microchannel cross-section could favor flow of one component or flow in one location over another. Differences in the viscosity and surface wettability of the healing agents also affect flow into the crack plane. A biologically-inspired solution in the form of an actively controlled pumping system has significant potential to improve flow of healing agents, promote mixing, prevent blockages from forming in microchannels and greatly extend the number of healing cycles in future generations of vascularized materials.

In summary, we have utilized synthetic microvascular networks to transport healing agents to sites of internal damage within a bulk material. Samples continued healing through as many as 13 cycles of damage and healing before succumbing to the gradual obstruction of healing agents caused by polymer formed in the crack plane. These experiments establish the efficacy of incorporating synthetic vascular networks within bulk

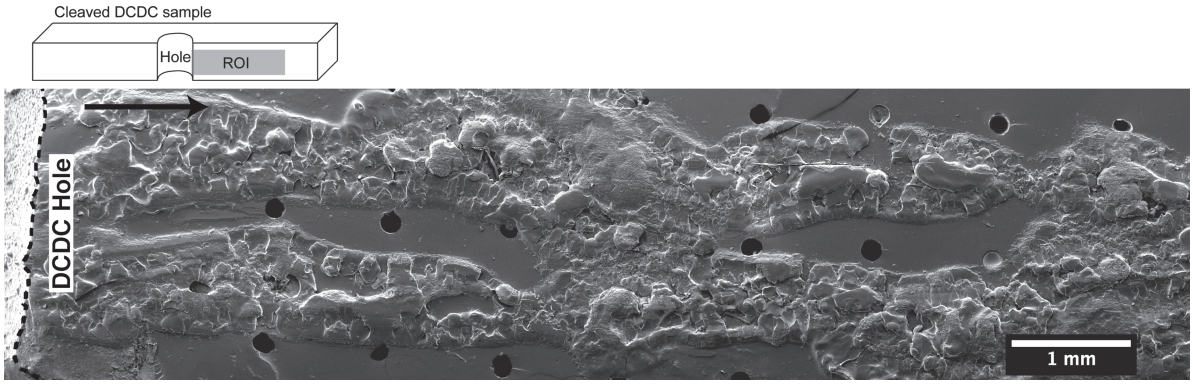

Figure 4. Scanning electron micrograph of the fracture surface of a self-healing sample showing coverage of healed polymer film in the crack plane after 10 cycles of damage and healing.

structural materials, rather than isolating vasculature within secondary materials with little or no structural role, and with limited access to the sites of structural damage. Further extension of healing cycles may be possible through active pumping of healing agents to the crack plane.

Experimental Section

Sample Preparation: Microvascular DCDC samples were fabricated by depositing a dual-ink structure into a silicon rubber mold via direct-ink writing. The structure consisted of a secondary fugitive ink (green, in Figure S1) that served as a support for the primary fugitive ink (white, in Figure S1) that served as a template for the microchannels. These dual-ink structures were infiltrated with an epoxy matrix (Epon™ 828 plus 40 pph Epikure™ 3274), which was allowed to cure for 24 hours at room temperature. The secondary fugitive ink was removed by dissolution in a water bath. The resulting spaces left within the sample by the secondary ink were backfilled with the same epoxy matrix material. After the backfilled epoxy cured, the primary fugitive ink was removed by heating to ~90 °C (above the ink's melting point, ~65 °C) and applying a slight vacuum. The triblock-copolymer and wax inks described by Hansen et al.[7] were used as the secondary and primary fugitive inks, respsectively. Direct-ink writing was performed using an Aerotech Inc. model ABL900 three-axis robotic deposition stage fitted with syringe barrels (HP7X from EFD Inc.) for extrusion of the fugitive inks. The inks were extruded through 27 gauge (200 μm) stainless steel dispensing tips from EFD Inc.

Microchannels in the final part were arranged into five independent layers distributed through the thickness of the sample. Each layer consisted of eight interconnected microchannels equally spaced at 1 mm intervals along the loading axis of the sample.

Experimental Protocol: Virgin (unfractured) samples were compressed on a screw-driven load frame under displacement control. Images were acquired and optical crack length measurements were recorded in real time. Samples were loaded until the cracks had propagated through all of the microchannels and were approximately 3 mm from the end of the sample. Healed samples were loaded under the same conditions as virgin samples.

After fracture, samples were placed on their sides, with the crack plane horizontal, in a 30 °C oven for 48 h to allow the healing agents time to react and cure. These modest curing conditions accelerate the reaction and expedite testing of the healed samples.[6] The supply of healing agents within the vasculature was maintained by manually recharging the microchannels with a syringe just prior to fracture testing. The recharging was timed to insure that if any healing agent was forced into the crack plane, there would not be sufficient time for the injected fluid to react and affect the heal test. Microchannels were left open to atmospheric pressure to allow equilibration of pressure after flow of healing agents.

Supporting Information

Supporting Information is available from the Wiley Online Library or from the author.

Acknowledgements

This work has been supported by the Air Force Office of Scientific Research Multidisciplinary University Research Initiative (grant F49550-05-1-0346). We wish to thank our colleagues in the Autonomous Materials Systems Group, especially Prof. J. S. Moore, Prof. J. A. Lewis, Prof. K. S. Toohey, Dr. B. J. Blaiszik and C. J. Hansen for their contributions to this work. We are also grateful to the Imaging Technology Group at the Beckman Institute for their imaging expertise and use of their facilities.

Received: July 16, 2010
Revised: August 11, 2010
Published online: September 24, 2010

[1] B. J. Blaiszik, S. L. B. Kramer, S. C. Olugebefola, J. S. Moore, N. R. Sottos, S. R. White, *Annu. Rev. Mater. Res.* **2010**, *40*, 179.
[2] K. S. Toohey, N. R. Sottos, J. A. Lewis, J. M. Moore, S. R. White, *Nat. Mater.* **2007**, *6*, 581.
[3] K. S. Toohey, N. R. Sottos, S. R. White, *Exp. Mech.* **2009**, *49*, 707.
[4] D. Therriault, S. R. White, J. A. Lewis, *Nat. Mater.* **2003**, *2*, 265.
[5] J. A. Lewis, *Adv. Funct. Mater.* **2006**, *16*, 2193.
[6] K. S. Toohey, C. J. Hansen, J. A. Lewis, S. R. White, N. R. Sottos, *Adv. Funct. Mater.* **2009**, *19*, 1399.
[7] C. J. Hansen, W. Wu, K. S. Toohey, N. R. Sottos, S. R. White, J. A. Lewis, *Adv. Mater.* **2009**, *21*, 1.
[8] H. R. Williams, R. S. Trask, I. P. Bond, *Smart. Mater. Struct.* **2007**, *16*, 1198.
[9] H. R. Williams, R. S. Trask, I. P. Bond, *Compos. Sci. Technol.* **2008**, *68*, 3171.
[10] C. Y. Huang, R. S. Trask, I. P. Bond, *J. R. Soc., Interface* **2010**, *7*, 1229.
[11] R. S. Trask, I. P. Bond, *J. R. Soc., Interface* **2010**, *7*, 921.
[12] H. R. Williams, R. S. Trask, A. C. Knights, E. R. Williams, I. P. Bond, *J. R. Soc., Interface*, **2008**, *5*, 735.

[13] R. S. Trask, H. R. Williams, I. P. Bond, *Bioinspiration Biomimetics*, **2007**, *2*, 1.
[14] H. R. Williams, R. S. Trask, P. M. Weaver, I. P. Bond, *J. R. Soc., Interface*, **2008**, *5*, 55.
[15] R. Carano, E. Filvaroff, *Drug Discovery Today* **2003**, *8*, 980.
[16] A. Chamay, P. Tschantz, *J. Biomech.* **1972**, *5*, 173.
[17] P. Fratzl, R. Weinkamer, *Prog. Mater. Sci.* **2007**, *52*, 1263.
[18] O. Pearson, D. Lieberman, *Yearb. Phys. Anthropol.* **2004**, *47*, 63.
[19] D. R. Carter, *J. Biomech.* **1987**, *20*, 1095.
[20] K. J. Koester, A. J. Ager, R. O. Ritchie, *Nat. Mater.* **2008**, *7*, 672.
[21] S. N. Crichton, M. Tomozawa, J. S. Hayden, T. I. Suratwala, J. H. Campbell, *J. Am. Ceram. Soc.* **1999**, *82*, 3097.
[22] T. A. Jenne, W. D. Keat, M. C. Larson, *Eng. Fract. Mech.* **1974**, *70*, 1697.
[23] T. A. Plaisted, A. V. Amirkhizi, S. Nemat-Nasser, *Int. J. Fract.* **2006**, *141*, 447.
[24] T. A. Plaisted, S. Nemat-Nasser, *Acta Mater.* **2007**, *55*, 5684.
[25] N. M. Marieb, K. Hoehn in *Human Anatomy and Physiology*, Pearson Benjamin Cummings, San Francisco, CA **2007,** p. 183.